**Supporting Information for**

# Thermal induced chemical cross-linking reinforced fluorinated polyurethane/polyacrylonitrile/polyvinyl butyral nanofibers for waterproof-breathable application

Junlu Sheng,[a] Min Zhang,[a] Wenjing Luo,[b] Jianyong Yu*[ac] and Bin Ding*[ac]

[a] *Key Laboratory of Textile Science & Technology, Ministry of Education, College of Textiles, Donghua University, Shanghai 201620, China*

[b] *Department of Occupational and Environmental Health, School of Public Health, Fourth Military Medical University, Xi'an, Shanxi 710032, China*

[c] *Nanofibers Research Center, Modern Textile Institute, Donghua University, Shanghai 200051, China*

* Corresponding author at: College of Textiles, Donghua University, Shanghai 201620, China.

Fax: +86 21 62378202.

*E-mail*: binding@dhu.edu.cn and yujy@dhu.edu.cn

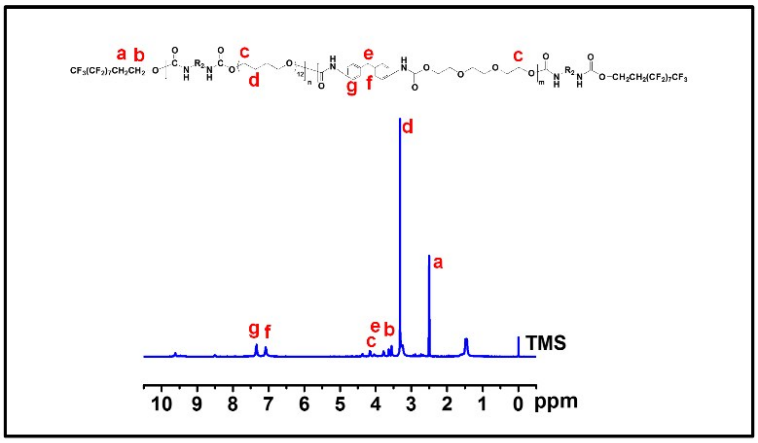


**Fig. S1** $^{1}$H NMR spectrograph of FPU

The FPU was subjected to NMR spectroscopic analysis after purification and crystallization. Fig. S1 presents the chemical structure and $^{1}$H NMR spectrum of FPU. The chemical shifts for -$CH_2$-$CH_2$- in terminal fluorinate segments appear at 2.49 and 3.51 ppm (Fig. S1a and b). For PTMEG and TEG segments, the shifts for -O-$CH_2$- and -$CH_2$-$CH_2$- appear at 3.73 and 3.32 ppm, respectively, as shown in Fig. S1c and d. The signals for aromatic protons of MDI groups appear between 7.10 to 7.37 ppm and for -$CH_2$- appears at 3.65 ppm (Fig. S1e-g).

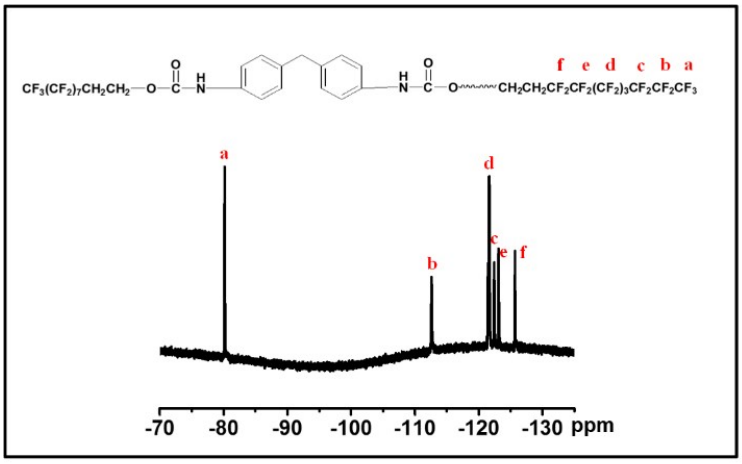


**Fig. S2** [19] F NMR spectrograph of FPU

[19]F NMR has given further structural affirmation of FPU (Fig. S2). The chemical shift for terminal $CF_3$ appears at 80.04 ppm (Fig. S2a), while for -$CF_2$-$CH_2$- appears at 126.77 ppm (Fig. S2f). The remaining -$CF_2$- has given their chemical shift between 112.58 to 123.72 ppm (Fig. S2b-e). The results from NMR analysis has confirmed the chemical structure of FPU.

**Table S1** Compositions and properties of various electrospinning solutions

| Samples | PVB (wt%) | BIP (wt%) | Viscosity (mPa*s) | Surface tension (mN/m) | Conductivity (μS/cm) |
|---|---|---|---|---|---|
| FPAN/PVB-50/BIP-0 | 50 | 0 | 2675 | 25.6 | 15.7 |
| FPAN/PVB-50/BIP-10 | | 10 | 2640 | 24.7 | 15.1 |
| FPAN/PVB-50/BIP-20 | | 20 | 3294 | 24.6 | 14.7 |
| FPAN/PVB-50/BIP-30 | | 30 | 3357 | 24.4 | 14.4 |
| FPAN/PVB-50/BIP-40 | | 40 | 3597 | 24.8 | 13.8 |
| FPAN | 0 | | 4324 | 20.1 | 31.0 |
| FPAN/PVB-25/BIP-30 | 25 | 30 | 3886 | 24.2 | 21.9 |
| FPAN/PVB-75/BIP-30 | 75 | | 2626 | 24.5 | 7.0 |

**Table S2** Average fiber diameter, $\lambda_{max}$ and porosity of the relevant nanofibrous membranes

| Samples | PVB (wt%) | BIP (wt%) | Average fiber diameter (nm) | $\lambda_{max}$ (μm) | Porosity (%) |
|---|---|---|---|---|---|
| FPAN/PVB-50/BIP-0 | 50 | 0 | 241±31 | 0.98 | 46±1.3 |
| FPAN/PVB-50/BIP-10 | | 10 | 291±25 | 1.02 | 59±1.5 |
| FPAN/PVB-50/BIP-20 | | 20 | 330±28 | 1.05 | 49±1.8 |
| FPAN/PVB-50/BIP-30 | | 30 | 419±36 | 1.28 | 45±1.5 |
| FPAN/PVB-50/BIP-40 | | 40 | 634±40 | 1.50 | 32±1.2 |
| FPAN | 0 | 30 | 387±31 | 1.69 | 85±2.6 |
| FPAN/PVB-25/BIP-30 | 25 | | 408±47 | 1.63 | 78±3.8 |
| FPAN/PVB-75/BIP-30 | 75 | | 601±79 | 1.06 | 30±4.9 |

**Table S3 Contact angle hysteresis of the dry-casting films fabricated from various polymers solutions.**

| Samples | FPAN/PVB-50/BIP-0 | FPAN/PVB-50/BIP-10 | FPAN/PVB-50/BIP-20 | FPAN/PVB-50/BIP-30 | FPAN/PVB-50/BIP-40 | FPAN | FPAN/PVB-25/BIP-30 | FPAN/PVB-75/BIP-30 |
|---|---|---|---|---|---|---|---|---|
| **PVB (wt%)** | | | 50 | | | 0 | 25 | 75 |
| **BIP (wt%)** | 0 | 10 | 20 | 30 | 40 | | 30 | |
| **Contact angle hysteresis (°)** | 8.5±1.1 | 10.7±1.4 | 9.4±1.6 | 12.7±2.2 | 12.3±2.4 | 8.6±1.7 | 12.6±1.3 | 9.5±1.2 |